



# Chromatin Remodeling Factor SMARCA5 is Essential for Hippocampal Memory Maintenance *via* Metabolic Pathways in Mice

Yu Qu<sup>1</sup> · Nan Zhou<sup>2</sup> · Xia Zhang<sup>1,3,4,5</sup> · Yan Li<sup>2</sup> · Xu-Feng Xu<sup>1,3</sup>

Received: 3 June 2022 / Accepted: 27 September 2022 / Published online: 18 February 2023

© Center for Excellence in Brain Science and Intelligence Technology, Chinese Academy of Sciences 2023, corrected publication 2023

**Abstract** Gene transcription and new protein synthesis regulated by epigenetics play integral roles in the formation of new memories. However, as an important part of epigenetics, the function of chromatin remodeling in learning and memory has been less studied. Here, we showed that SMARCA5 (SWI/SNF related, matrix-associated, actin-dependent regulator of chromatin, subfamily A, member 5), a critical chromatin remodeler, was responsible for hippocampus-dependent memory maintenance and neurogenesis. Using proteomics analysis, we found protein expression changes in the hippocampal dentate gyrus (DG) after the knockdown of SMARCA5 during contextual fear conditioning (CFC) memory maintenance in mice. Moreover,

SMARCA5 was revealed to participate in CFC memory maintenance *via* modulating the proteins of metabolic pathways such as nucleoside diphosphate kinase-3 (NME3) and aminoacylase 1 (ACY1). This work is the first to describe the role of SMARCA5 in memory maintenance and to demonstrate the involvement of metabolic pathways regulated by SMARCA5 in learning and memory.

**Keywords** Epigenetic regulation · SMARCA5 · Hippocampal memory · Chromatin remodeling · Metabolic pathway

Yu Qu and Nan Zhou contributed equally to this work.

**Supplementary Information** The online version contains supplementary material available at <https://doi.org/10.1007/s12264-023-01032-x>.

✉ Yan Li  
yanli@sdu.edu.cn

✉ Xu-Feng Xu  
Xuxufeng@qdu.edu.cn

<sup>1</sup> Institute of Neuropsychiatric Diseases, Qingdao University, Qingdao 266001, China

<sup>2</sup> Department of Urology, Qilu Hospital of Shandong University, Jinan 250012, China

<sup>3</sup> University of Ottawa Institute of Mental Health Research at the Royal, Ottawa K1Z7K4, Canada

<sup>4</sup> Department of Anesthesiology and Perioperative Medicine, Xijing Hospital, Fourth Military Medical University, Xi'an 710032, China

<sup>5</sup> Key Laboratory of Modern Teaching Technology & College of Life Sciences, Shaanxi Normal University, Xi'an 710062, China

## Introduction

Memory allows us to access information from the world and store it in the brain. Unraveling the mechanisms underlying memory formation and consolidation has been a major goal of the field of neuroscience for decades. Recent studies have found that epigenetic regulation plays an indispensable role in learning and memory by modifying histones and DNA to regulate gene expression and new protein synthesis [1–3]. Epigenetic regulation of the genome involves processes such as non-coding RNA, DNA methylation, histone methylation and acetylation, and chromatin remodeling [4]. Among these, there have been a large number of reports on the functions of non-coding RNA in learning and memory [5–9]. The functions of DNA methylation, histone methylation, and acetylation-related proteins in learning and memory have also been reported by many studies [10–13]. In contrast, although studies have shown that some chromatin remodeling factors are involved in the processes of learning and memory [14, 15], the functions of most chromatin remodeling factors remain unclear.

The SWI/SNF related, matrix-associated, actin-dependent regulator of chromatin, subfamily A, member 5

(SMARCA5) protein is a member of the SWI/SNF family; it has helicase and ATPase activities and is thought to regulate the transcription of certain genes by altering the chromatin structure around those genes. Studies have shown that SMARCA5 promotes tumor growth in ovarian cancer and glioma [16, 17]. *In vivo*, SMARCA5 is highly expressed in the brain and its conditional knockout reduces progenitor expansion and dendritic arborization, resulting in severe cerebellar and forebrain hypoplasia [18–20]. A recent study revealed that SMARCA5 expression in the amygdala and ventral hippocampus is reduced in mice displaying high anxiety-related behavior [21], suggesting that SMARCA5 plays an important role in higher brain functions such as emotion or learning and memory. However, up to now, the functions and mechanisms of SMARCA5 in learning and memory remain unclear.

In this study, we employed neuropharmacological, behavioral, immunochemical, BrdU administrative, and proteomic methods in combination with the Gene Ontology (GO) and Kyoto Encyclopedia of Genes and Genomes (KEGG) analysis, to examine whether and how the SMARCA5 participates in the modulation of hippocampus-dependent memory. Surprisingly, we observed SMARCA5 participated in CFC memory maintenance *via* modulating the proteins of metabolic pathways such as nucleoside diphosphate kinase-3 (NME3) and aminoacylase 1 (ACY1).

## Materials and Methods

### Animals

Adult C57BL/6J mice (2–3 months old, Vital River Laboratories) were singly housed in standard mouse cages in a temperature-controlled room ( $22 \pm 2$  °C) under diurnal conditions (12 h light/dark cycle) with food and water available *ad libitum*. All animal procedures were in accordance with the guidelines of the National Institutes of Health Guide for the Care and Use of Laboratory Animals and were approved by the Institutional Animal Care and Use Committee of Qingdao University.

### Tissue Isolation

Tissue was isolated as in previous studies [22–25]. The ventral hippocampus (VH) was defined as AP: –2.46 to –3.80 mm, the dorsal hippocampus (DH) was defined as AP: –0.94 to –2.30 mm, and the amygdala (Amy) was defined as AP: –0.59 to –2.45 mm. The mouse brains were removed and then placed in a mouse brain slicer (Braintree Scientific, Braintree, Massachusetts, United States). Coronal sections

(1 mm thick) were collected and the above tissues were isolated under a dissecting microscope following the mouse brain atlas. The tissues were dissected on ice and stored at –80 °C until use.

### Western Blot

Different hippocampal regions were isolated at 0 °C and then homogenized in a Bullet Blender Homogenizer (Next Advance, New York City, USA). The homogenates were placed in a pH 7.5 Tris-HCl buffer containing 1% NP-40, 1 mmol/L EDTA, 150 mmol/L NaCl, 1 µg/mL leupeptin, 3.8 µg/mL aprotinin, 1 µg/mL pepstatin, 1 mmol/L PMSF, 1 mmol/L Na<sub>3</sub>VO<sub>4</sub>, and 2 mmol/L NaF. The extracts were clarified by centrifugation at 4 °C (14,000× g for 20 min). Supernatants were gathered and eluted with an SDS sample buffer, and proteins were resolved by SDS-PAGE. Rabbit anti-SMARCA5 antibody (abs115900, 1:1000; Absin Bioscience, Shanghai, China), rabbit anti-ACY1 antibody (Absin, abs117091, 1:1000), mouse anti-α-tubulin (Sigma-Aldrich, Saint Louis, USA, T6199, 1:10000), and rabbit anti-NME3 antibody (Absin, abs153616, 1:1000) were separately used as primary antibodies. Goat anti-rabbit or anti-mouse secondary antibodies (Calbiochem, San Diego, USA, 1:1000) were used to react with the corresponding primary antibodies. Immunoreactive bands were visualized by enhanced chemiluminescence (Pierce ECL, Thermo Fisher Scientific, Waltham, USA). Densitometric analysis of the bands was calculated by Quantity One (version 4.6.2, Bio-Rad, Hercules, USA).

### RT-PCR

Total RNA was isolated using TRIzol-A<sup>+</sup> RNA isolation reagent (Tiangen, Beijing, China), following the manufacturer's protocol. A 0.5 µg aliquot of each sample was treated with DNase to avoid DNA contamination and then was reverse-transcribed using the ReverTra Ace qPCR RT Kit (catalog #FSQ-101; Toyobo, Osaka, Japan) according to the manufacturer's instructions. Quantitative real-time RT-PCR was performed in a Cycler (Bio-Rad) using SYBR-Green (Roche, Basel, Switzerland). The primer sequences used are listed in Table 1. Each sample was assayed in duplicate and the levels of miRNA were normalized for each well to the β-actin levels using  $2^{-\Delta\Delta CT}$ .

### Surgery and Microinjection

Under anesthesia with isoflurane (4% for induction, 1.5% for maintenance), each adult mouse was placed in a stereotaxic

**Table 1** List of primer pairs used for RT-PCR

SMARCA5	F: CGACAATGCATCCGAAACTCC	R: ACCGTCCATCTTACGTTTCTGTG
HAGH	F: CCTGGGCTGAAGGTTTATGGAG	R: CCGAAGTATGGCAGGGTGTG
POMGNT2	F: GACGGTTACAGTGTCCCTGGAG	R: GCATGCTGACCAACATGGAG
MIF	F: GAGGGGTTTCTGTCCGAGC	R: GTTCGTGCCGCTAAAAGTCA
HMOX2	F: ATGTGGACAATGCCAGCAA	R: CAGCCTGGTCCAGTTCCTGAATA
NT5C	F: CGGACCTGGCGGAAAAAGT	R: GTCGTTTCATCTCTCGCAAAGC
NME3	F: GAGATCGTGCGTCGCTTGA	R: CGCAGCTCGACATAATGCTC
HMGCS1	F: GGTTAGCTGTAATCACGTGAGCAGA	R: GTCCACAACGCCAGGTGTA
ACY1	F: CTGCAGAGATGGTGCCAGGA	R: GGGTGTTCATTCGAGGCTCTGTA
SCP2	F: CTACCTGGGTGGTGGATGTGAAG	R: GTCTGAGTCGGCCATGGTGA
GATB	F: CACTGAACCTGAGAATGGAGGTGAA	R: CAGGTTGGGCTCTGGCATAA
ADK	F: ACCTTGACCTGGAGCGGAAC	R: CAGCATAGCGAGCCACTTTCAATA
NT5C3	F: GATCCTGTTCTCACCGTGAAG	R: CGTGCTGTTGAAGTTTACCGAAG
ATP5PB	F: AACATGATGCGTCGCAAGGA	R: CAATGCACTTGGCAATGGTCTC
ADCY5	F: TGCCAACACCAGTGGGTTC	R: ACTGCACGCTGTCACCAGTC
NDUFV3	F: ATTTGTGCCATGGCGGTCT	R: CCTTTGCACTTCTCTGACTCTGT

apparatus (8001, RWD Life Science, Shenzhen, China) before the surgery. The coordinates (in mm, with reference to bregma) were as follows: lateral (L),  $\pm 1.0$ ; anteroposterior (AP),  $-1.70$ ; and dorsoventral (V),  $-2.3$ . The AAV-virus or lentivirus with green-fluorescent protein sequence was injected bilaterally into DG by microinjection (KD Scientific, CA, USA). Infusions were performed at a volume of  $0.1 \mu\text{L}$  for 3 min and the infusion cannula was left for diffusion for an additional 3 min. All viruses were purchased from GeneChem Co. (Shanghai, China) and the AAV9 serotype was used to package the AAV interference and overexpression virus. GV388 vectors (CMV bGlobin-MCS-EGFP-3FLAG-WPRE-hGH polyA) were used to package the mouse ACY1 and NME3 overexpression AAV-virus. GV478 vectors (U6-MCS-CAG-EGFP) were used to package the mouse interference AAV-virus. GV492 (Ubi-MCS-3FLAG-CBh-gcGFP-IRES-purpmycin) vectors were used to package the Samra5 overexpression lentivirus. The SMARCA5 shRNA sequence used for si-SMARCA5 AAV-virus was as follows: SMARCA5 shRNA antisense, 5' ACCAGATGTGTTAATTCAGC 3'; The ACY1 shRNA sequence used for si-ACY1 AAV-virus was as follows: ACY1 shRNA antisense, 5' TGAAGAGTGTGTCAGCATCCAGT 3'; The NME3 shRNA sequence used for si-NME3 AAV-virus was as follows: NME3 shRNA antisense, 5' GGTGCTGACCATCTT TGCTAA 3'. The unit titer of SMARCA5-OE lentivirus was  $1 \times 10^8$  transduction units (TU)/mL. The unit titer of AAV-virus was  $1 \times 10^{13}$  TU/mL.

## Behavior

The behavioral experiments were conducted as in previous studies [26].

## Contextual Fear Conditioning (CFC)

On the first day, mice were put into a standard fear-conditioning chamber (Panlab, Boston, USA) for training. Each mouse was left in the conditioning context for 2 min, at the end of which, three shocks ( $0.4$  or  $0.7$  mA for 1 s) were delivered with an inter-trial interval of 59 s. After the last shock, each mouse was left in the chamber for 59 s before being moved back to its home cage. 1 h and 24 h after training, each mouse was returned to the conditioning chamber where training occurred and the freezing responses were recorded for 5 min without foot shock.

## Morris Water Maze

The apparatus consisted of a circular water tank (120 cm diameter, 40 cm height) filled with water ( $22^\circ\text{C}$ ) to a depth of 25 cm, and the water was made opaque by adding non-toxic white powder paint. A circular escape platform (6 cm in diameter) was placed 1 cm below the water surface. During the period of learning, the platform was always placed in the center of the same quadrant (target quadrant). Each trial consisted of a maximum of 60 s starting from one of the four quadrants with the mouse facing the wall. If a mouse could not reach the platform in 60 s, it was guided to the platform. After reaching the platform, mice were allowed to stay there for 30 s, and then quickly dried with a towel and put under a heating lamp set at exactly  $37^\circ\text{C}$  to avoid hypothermia. Each mouse received four trials per day in the water maze on each of the five training days. In the learning process, the escape latencies for a single day were averaged to produce a daily mean. On day 6, the platform was removed, and each mouse was allowed to swim for 60 s. The number

of platform crossings and the time spent in each of the four quadrants by each mouse were recorded with a video tracking system (Smart, Panlab).

### Novel Object Recognition Test

The experimental device was composed of a square test box and two identical test objects that were mouse-sized or only slightly larger to encourage exploration. The objects used were fairly simple but had a few distinguishing features. The test objects were screened before the experiment to determine whether the mice have a similar preference for them. The test was divided into an adaptation period, a training period, and a test period. During the adaptation period, each mouse was placed in the middle of the test box, without objects. They were allowed to move freely for 10 min to get familiar with the environment. 24 h later, two identical objects A were placed on both sides of the same side wall of the test box. The mice were placed in the test box, and the exploration time spent on each object was recorded. When the mouse's mouth was close to the object within 2 cm, the time for the mouse to climb on or walk around the object was also included. The total activity time of mice in the box was 10 min. 24 h later, one familiar object, A, was changed to a novel object, B, and mice were exposed to both objects A and B for 3 min. The exploration time for object A (TA) or B (TB) was recorded in a single-blind trial by an observer blind to the treatment status of mice to exclude observer bias. The recognition index, which is calculated by  $TB/(TA + TB)$ , was reflected as the recognition memory of mice. Total exploration time was also analyzed to assess the motor ability of mice.

### BrdU Administration

As shown in Fig. 4A, to analyze cell proliferation in animals, the mice were sacrificed 2 h after intraperitoneal (i.p.) injection of bromodeoxyuridine (BrdU) (Sigma-Aldrich, B5002, 50 mg/kg) in 0.9% NaCl solution.

### Immunocytochemistry

Mice were anesthetized with 5% chloral hydrate anesthesia (8 ml/kg, i.p.) and perfused with 0.9% NaCl, followed by 4% paraformaldehyde (PFA), pH 7.6. Their brains were post-fixed in 4% PFA overnight, followed by equilibration at 4 °C in 30% sucrose for another 24 h before sectioning. Then the brains were cut into a series of 40 µm coronal sections on a Microm cryostat (HM 550) at −20 °C. For BrdU detection, sections were pretreated with 50% formamide/2

×SSC (Saline-Sodium Citrate buffer) for 1 h at 55 °C, and then the sections were rapidly washed in 2 × SSC. After this, the sections were incubated with 2 N HCl for 30 min at 37 °C and washed in 0.1 mol/L borate buffer, pH 8.5, for 10 min. After blocking with 10% donkey serum in phosphate-buffered saline containing 0.3% Triton X-100 for 1 h, the sections were incubated with primary antibodies to BrdU (Abcam, Cambridge, UK, 1:1000) overnight at 4 °C, followed by Alexa Fluor secondary antibodies for 1 h.

### Imaging and Quantification

BrdU-positive (BrdU<sup>+</sup>) cells within the granule cell layer of the DG were imaged by confocal fluorescence microscopy with a Carl Zeiss LSM-780 microscope fitted with a standard (1 Airy disk) pinhole and standard filter sets (Microstructural Platform of Shandong University, Jinan, China). The MetaMorph software package (Molecular Devices, Sunnyvale, USA) with an unbiased stereological protocol as previously described was used to count [27, 28]. Briefly, we counted the BrdU<sup>+</sup> cells in the DG in every sixth section throughout the rostrocaudal extent of the DG. This ensured the same cell was not counted repeatedly. Sections were imaged at 20× throughout the rostral-caudal extent of the DG with projections of 12–15 Z planes taken at 2-µm intervals. The total number of BrdU<sup>+</sup> cells was multiplied by six to estimate the total number in the whole DG. The data are presented as the number of cells per cubic millimeter.

### Proteomics Analysis

The flow of this experiment is shown in Fig. 5A. Briefly, mice were injected with the control or si-SMARCA5 AAV-virus into the DG area. Four weeks later, both groups received CFC training. Two hours after the CFC training, mice were sacrificed and the DG regions were quickly obtained at 0 °C and placed in liquid nitrogen. The control group and the si-SMARCA5 group each had three replicate samples, where each sample contained the DG regions of four mice. Proteomics analysis was completed by GeneChem Co.

### Statistics

CFC training and Morris water maze training data were analyzed by repeated measures two-way ANOVA. Other group differences were analyzed using a two-tailed *t* test or one-way ANOVA, which was followed by Bonferroni *post hoc* analysis to compare means from several groups simultaneously. Significance was set at  $P < 0.05$ . Results are



expressed as the mean  $\pm$  SEM. Data analyses were applied using GraphPad Prism version 8.0 (GraphPad Software, San Diego, USA).

## Results

### SMARCA5 is Upregulated in the Hippocampus after CFC Training

To determine whether SMARCA5 is involved in hippocampal-dependent memory, we initially used a commonly used hippocampus-dependent memory paradigm, CFC, to assess the changes of SMARCA5 expression in different regions of the hippocampus at different time points after CFC training (Fig. 1A). RT-PCR results showed that *SMARCA5* mRNA levels were significantly elevated in the dorsal DG, but not in the DG of the ventral hippocampal and BLA region, which started at 1 h and was sustained to 4 h (Fig. 1B, C, D; dorsal DG:  $F_{(6,33)} = 20.68$ ,  $P < 0.001$ ; ventral DG:  $F_{(6,33)} = 2.481$ ,  $P = 0.0531$ ; BLA:  $F_{(6,33)} = 2.292$ ,  $P = 0.0585$ , one-way ANOVA). Western Blot results indicated that the SMARCA5 protein levels in the dorsal DG were significantly increased at 2 h and 4 h after CFC training (Fig. 1E, F;  $F_{(6,34)} = 18.51$ ,  $P < 0.001$ , one-way ANOVA), which suggested that SMARCA5 is involved in hippocampal fear memory. Next, we determined whether the CFC training-induced increase in SMARCA5 was specific to associative fear conditioning memory rather than exposure to either shock or context alone. Our results showed that, compared with the naive group, neither shock alone nor context alone upregulated the SMARCA5 mRNA and protein levels (Fig. 1G, H, I; mRNA:  $F_{(3,20)} = 30.54$ ,  $P < 0.001$ ; protein:  $F_{(3,20)} = 26.08$ ,  $P < 0.001$ , one-way ANOVA), suggesting that the enhanced SMARCA5 is specific to the associated CFC memory.

### Manipulation of SMARCA5 in the DG Affects the Long-term Memory Maintenance of CFC

Previous studies have revealed that conditional knockout of SMARCA5 severely impairs brain development [19], so we chose the SMARCA5-shRNA-AAV-virus (si-SMARCA5) or SMARCA5-overexpression-lentivirus (SMARCA5-OE) to knockdown or overexpress the SMARCA5 levels rather than using SMARCA5 conditional knockout mice. Si-SMARCA5 or SMARCA5-OE virus was injected stereotactically into the DG to investigate whether the upregulated SMARCA5 is functionally involved in hippocampal memory. Four weeks after virus injection, a huge number of GFP-positive neurons were observed in the DG, suggesting that the AAV-virus was successfully transfected into the DG (Fig. 2A).

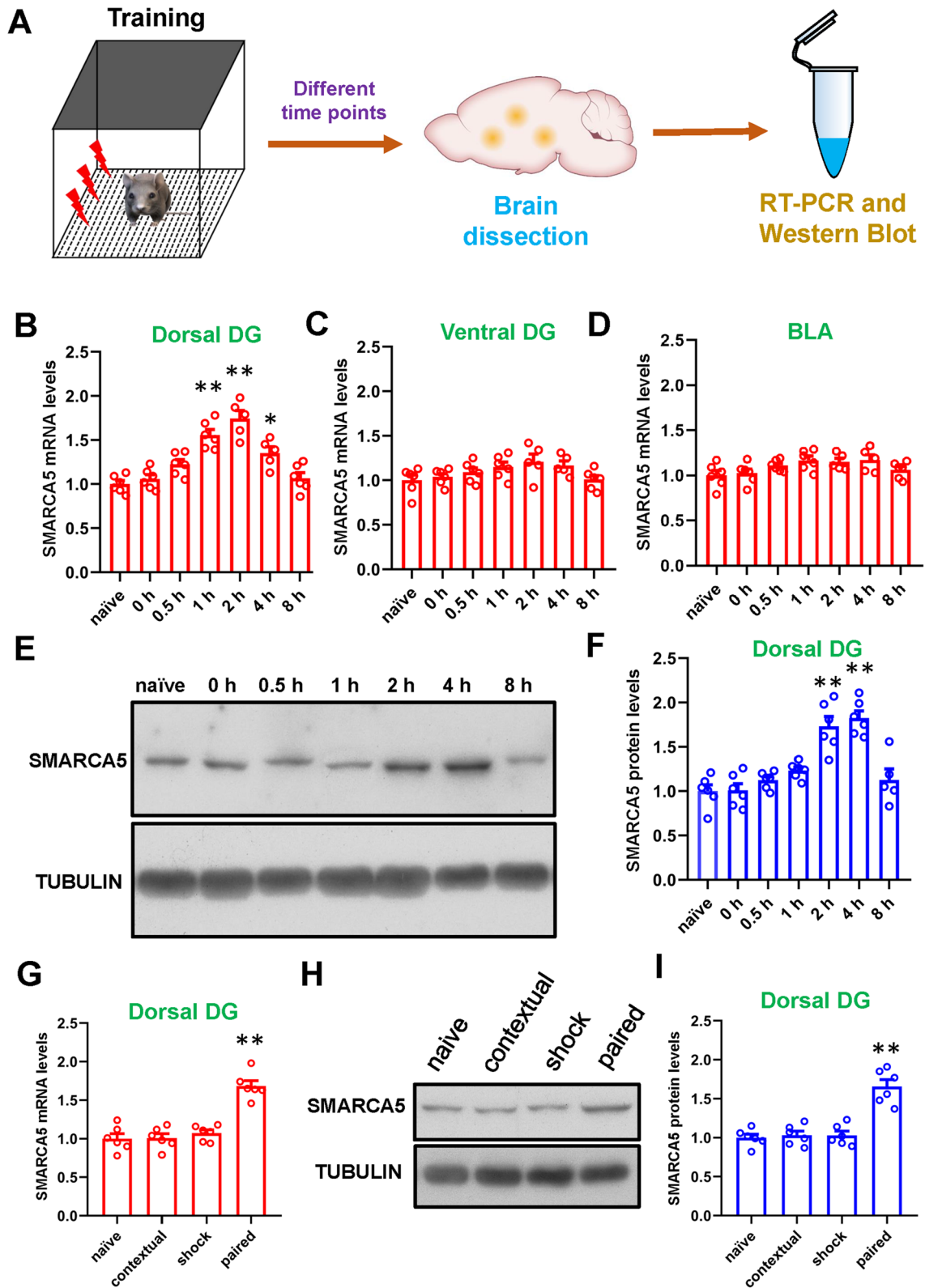
RT-PCR results showed that *SMARCA5* mRNA levels in DG were reduced to 53.8% after injection of si-SMARCA5 AAV-virus (Fig. 2B;  $P < 0.001$ , two-tailed *t* test), which suggested that the si-SMARCA5 virus effectively decreased the SMARCA5 levels in the DG. Moreover, the results showed that SMARCA5 levels in the DG were increased by 70.7% after SMARCA5-OE lentivirus injection (Fig. 2B;  $P < 0.001$ , two-tailed *t* test). These results revealed that SMARCA5-OE lentivirus effectively enhanced the SMARCA5 expression.

Next, we evaluated the role of SMARCA5 in CFC memory by using CFC training and testing as shown in Fig. 2C. Our results showed that the si-SMARCA5 group exhibited a freezing time in the CFC training and short-term memory (STM) testing similar to the control group, which suggested that knockdown of SMARCA5 did not affect the contextual fear memory acquisition and STM formation (Fig. 2D, E). However, when we examined the long-term memory (LTM) maintenance of the contextual fear memory 24 h after training, mice in the si-SMARCA5 group had a lower freezing time than mice in the control group, suggesting that reducing SMARCA5 impairs the LTM maintenance of contextual fear memory (Fig. 2E;  $P < 0.001$ , two-tailed *t* test).

We then used SMARCA5-overexpression lentivirus to determine whether overexpressing SMARCA5 enhances the LTM maintenance of contextual fear memory. To avoid a ceiling effect, we used a weaker electric shock to condition the mice in the CFC training. Our results revealed that mice in both groups exhibited a similar freezing time during CFC training (Fig. 2F) and the STM test (Fig. 2G), suggesting that increasing the expression of SMARCA5 had no effect on the contextual fear memory acquisition and STM formation. However, in the LTM test, mice in the SMARCA5-OE group showed a significantly increased freezing time when compared with control group mice (Fig. 2G;  $P = 0.0037$ , two-tailed *t* test), which suggested that overexpression of SMARCA5 does enhance the LTM maintenance of contextual fear memory. Taken together, these results indicate that SMARCA5 is involved in the LTM maintenance of contextual fear memory.

### Knockdown of SMARCA5 Impairs Recognition Memory and Spatial Memory in the DG

We then subjected mice to a novel object recognition test and Morris water maze test to determine whether SMARCA5 is involved in other hippocampus-dependent memory types. Data demonstrated that mice in the si-SMARCA5 group exhibited locomotion similar to the mice in the control group (Fig. 3A, B), suggesting that blocking SMARCA5 expression does not affect spontaneous exploratory activity. However, mice in the si-SMARCA5 group showed a severe deficit in recognition memory when compared with the control



group (Fig. 3C;  $P = 0.0021$ , two-tailed  $t$  test), and both groups had a similar total exploration time (Fig. 3D), which suggested that SMARCA5 is essential for hippocampal

recognition memory. In the Morris water maze test, mice in the si-SMARCA5 group showed a significantly increased escape latency in the hidden platform trials (Fig. 3E;  $F_{(4,76)}$

**Fig. 1** SMARCA5 is upregulated in the hippocampus after CFC training. **A** Schematic of mouse brain dissection at different time points after CFC training. **B–D** The relative SMARCA5 mRNA levels in a different region of the hippocampus at different time points after CFC training. RT-PCR analysis (**B**) shows the relative SMARCA5 mRNA levels in CA1 at different time courses after CFC training ( $n = 5–6$  per group;  $**P < 0.01$  vs naive group). RT-PCR analysis (**C**) shows the relative SMARCA5 mRNA levels in CA3 at different time courses after CFC training ( $n = 5–6$  per group). RT-PCR analysis (**D**) shows the relative SMARCA5 mRNA levels in DG at different time courses after CFC training ( $**P < 0.01$  vs naive group,  $*P < 0.05$  vs naive group;  $n = 5–6$  per group). **E, F** Western Blot analysis shows the relative SMARCA5 protein levels in the DG at different time courses after CFC training ( $n = 5–6$  per group;  $**P < 0.01$  vs naive group). Representative immunoblots are shown in (**E**), and the relative densitometric analysis is shown in (**F**). **G** Relative mRNA levels of SMARCA5 in the hippocampus 2 h after context alone, the immediate shock alone, or paired CFC training normalized to control ( $n = 6$  per group;  $**P < 0.01$  vs naive group). **H, I** Relative protein levels of SMARCA5 in the hippocampus 2 h after context alone, the immediate shock alone, or paired CFC training normalized to control ( $n = 6$  per group;  $**P < 0.01$  vs naive group). Representative immunoblots are shown in (**H**), and the relative densitometric analysis is shown in (**I**). All values are presented as the mean  $\pm$  SEM.

$= 3.038$ ,  $P = 0.022$ , repeated measures two-way ANOVA), a decreased number of platform crossings (Fig. 3F;  $P = 0.002$ , two-tailed  $t$  test), and spent less time in the target quadrant during the probe test (Fig. 3G;  $P = 0.0062$ , two-tailed  $t$  test) in comparison to control group mice, which suggested that knockdown of SMARCA5 impairs hippocampus-dependent spatial memory.

Taken together, these results revealed that SMARCA5 is essential for hippocampus-dependent memory.

### SMARCA5 Is Involved in Hippocampal Neurogenesis in Adult Mice.

Studies have demonstrated that DG is one of the main loci for adult neurogenesis [29]. SMARCA5 has been demonstrated to be related to progenitor expansion as well as cerebellar and forebrain morphology during development [19]. We then investigated whether SMARCA5 affects adult neurogenesis in the DG. To this end, we used BrdU to label newborn cells and found that mice in the si-SMARCA5 group showed significantly fewer BrdU-positive cells than the control group (Fig. 4A, B, C;  $P = 0.0071$ , two-tailed  $t$  test). These results indicated that SMARCA5 knockdown reduces progenitor proliferation in the DG. Moreover, the number of BrdU-labeled cells in the SMARCA5-OE group was significantly higher than in the control group (Fig. 4B, C;  $P < 0.001$ , two-tailed  $t$  test), which suggested that SMARCA5 overexpression elevates hippocampal neural precursor cell proliferation. All in all, these results reveal that SMARCA5 is essential for adult hippocampal neurogenesis in the DG.

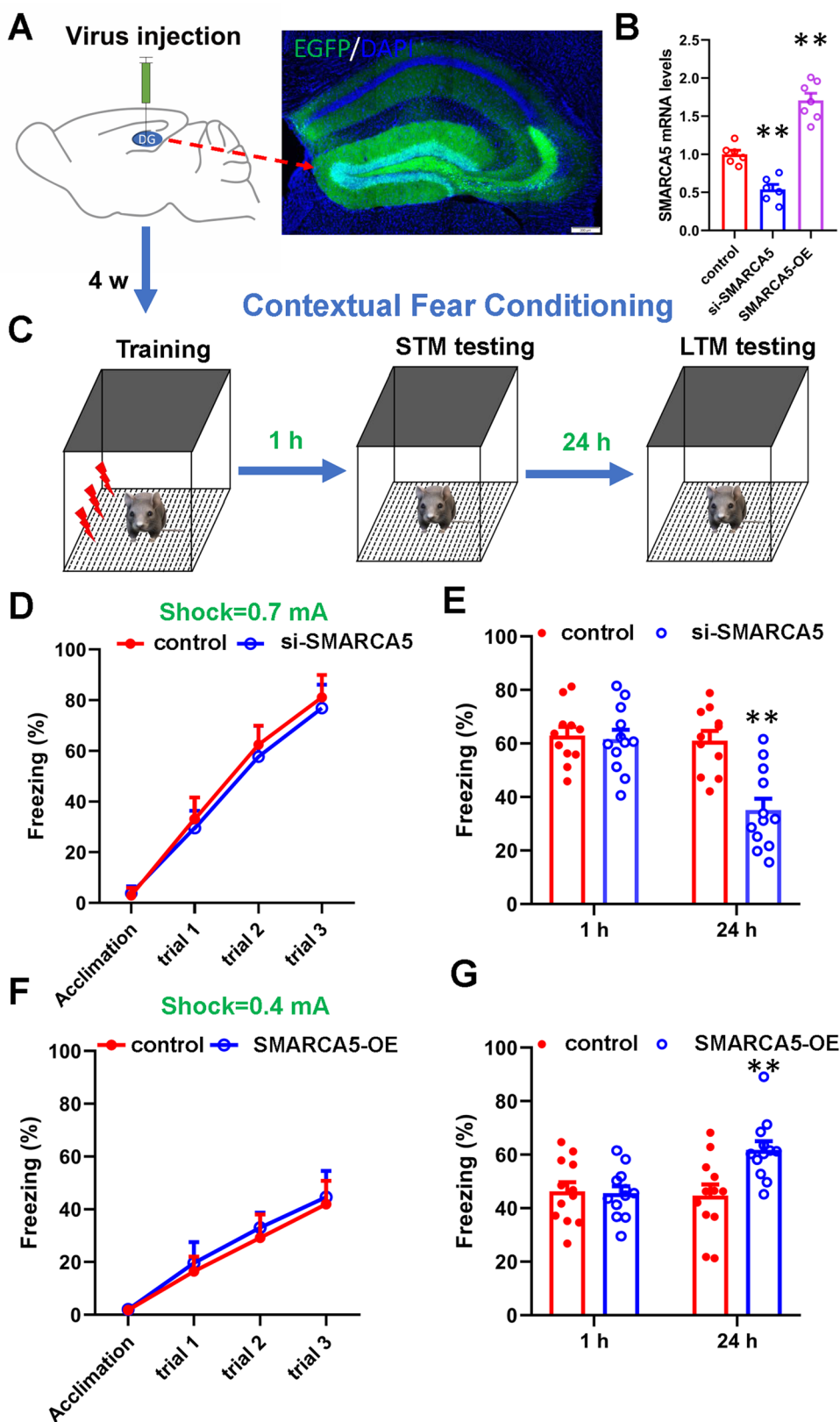
### Proteomics Analysis of the Effects of SMARCA5 Knockdown on Protein Changes in the DG after CFC Training.

The above data revealed that SMARCA5 is essential for adult hippocampal memory and neurogenesis, but the underlying mechanisms were still unclear. To investigate the proteins that are regulated by SMARCA5 in the CFC process, proteomics analysis was used to fulfill our aim. Following the experimental procedure illustrated in Fig. 5A, thousands of proteins were read by the proteomics analysis, of which the expression of 108 proteins in the si-SMARCA5 group was significantly different from the control group (supplementary data 1), suggesting that these 108 proteins could be modulated by SMARCA5 in the CFC process (Fig. 5B). Notably, among the 108 proteins, 39 were increased and the other 69 were decreased in the si-SMARCA5 group (Fig. 5C, D). We then applied protein subcellular localization analysis to investigate the spatial distribution of the 108 proteins in neurons (supplementary data 2). Our results demonstrated that 33.3% of the 108 proteins were localized in the cytosol, 22.2% in the nucleus, 17.6% in mitochondria, 14.8% in the plasma membrane, and the rest were in extracellular space (6.5%), the endoplasmic reticulum (3.7%), and the cytoskeleton (1.9%) (Fig. 5E). Moreover, proteomics analysis results revealed that the SMARCA5 protein level in the si-SMARCA5 group was lower than in the control group (Fig. 5F;  $P = 0.0031$ , two-tailed  $t$  test), which showed that injecting the si-SMARCA5 AAV-virus into the DG area effectively decreased the elevated SMARCA5 expression after CFC training in mice, and also indicated that the proteomics analysis result was relatively accurate.

### GO and KEGG Analysis to Determine the Signaling Pathways and Enrichment of the differentially-expressed proteins (DEPs)

To further analyze the 108 DEPs identified by proteomics, the Gene Ontology (GO) and Kyoto Encyclopedia of Genes and Genomes (KEGG) databases were used to classify and identify the signaling pathways to which these proteins belong and their enrichment in these signaling pathways. During GO analysis, the identified proteins were divided into three groups: biological process (BP), molecular function (MF), and cellular component (CC). In the BP category, the five most highly enriched proteins were associated with the cellular process, as well as a biological process, metabolic processes, developmental process, and response to stimulus (Fig. 6A, supplementary data 3). The main BP enrichment of DEPs was chorioallantoic fusion, regulation of protein localization, and skeletal muscle tissue development (Fig. 6B, supplementary data 3). In the MF category, the three highly

**Fig. 2** Manipulation of SMARCA5 in the DG affects the CFC long-term memory formation. **A** The location and diffusion range of the AAV-virus and lentivirus microinjected into the DG. Scale bar, 200  $\mu$ m. **B** Relative mRNA levels of SMARCA5 in the DG after si-SMARCA5 AAV-virus or overexpression lentivirus injection ( $n = 6-7$  per group;  $**P < 0.01$  vs control group). **C** Schematic of the CFC training and testing. **D, E** SMARCA5 knockdown impairs the contextual fear memory. **(D)** The freezing response during the training process. **(E)** The freezing response at 1 h and 24 h after training ( $n = 11-12$  per group;  $**P < 0.01$  vs 24 h control group). **F, G** SMARCA5 overexpression enhances the contextual fear memory with a weaker electric shock. The freezing response in the training process **(F)**. The freezing response at 1 h and 24 h after training ( $n = 12$  per group;  $**P < 0.01$  vs 24 h control group). All values are presented as the mean  $\pm$  SEM.



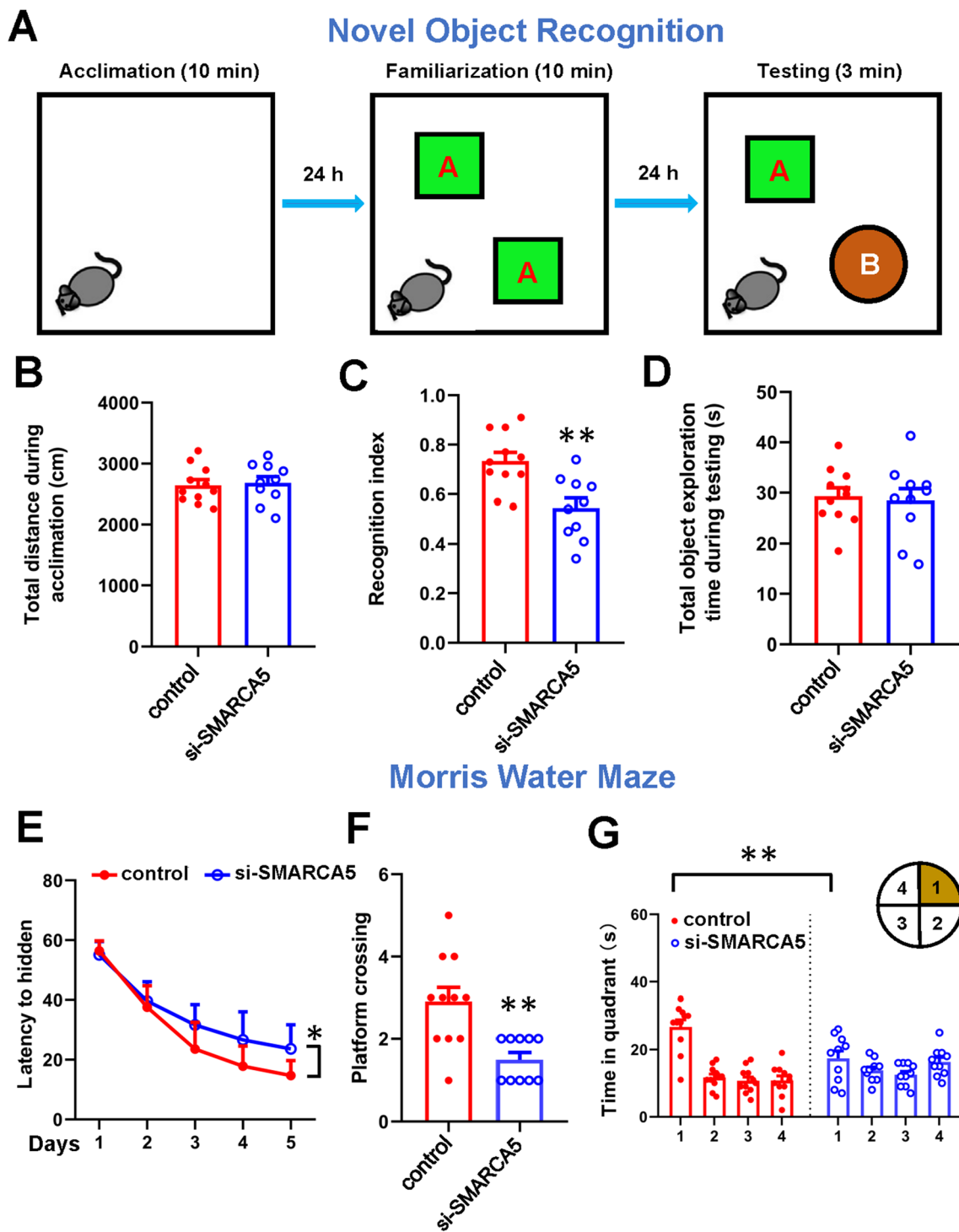
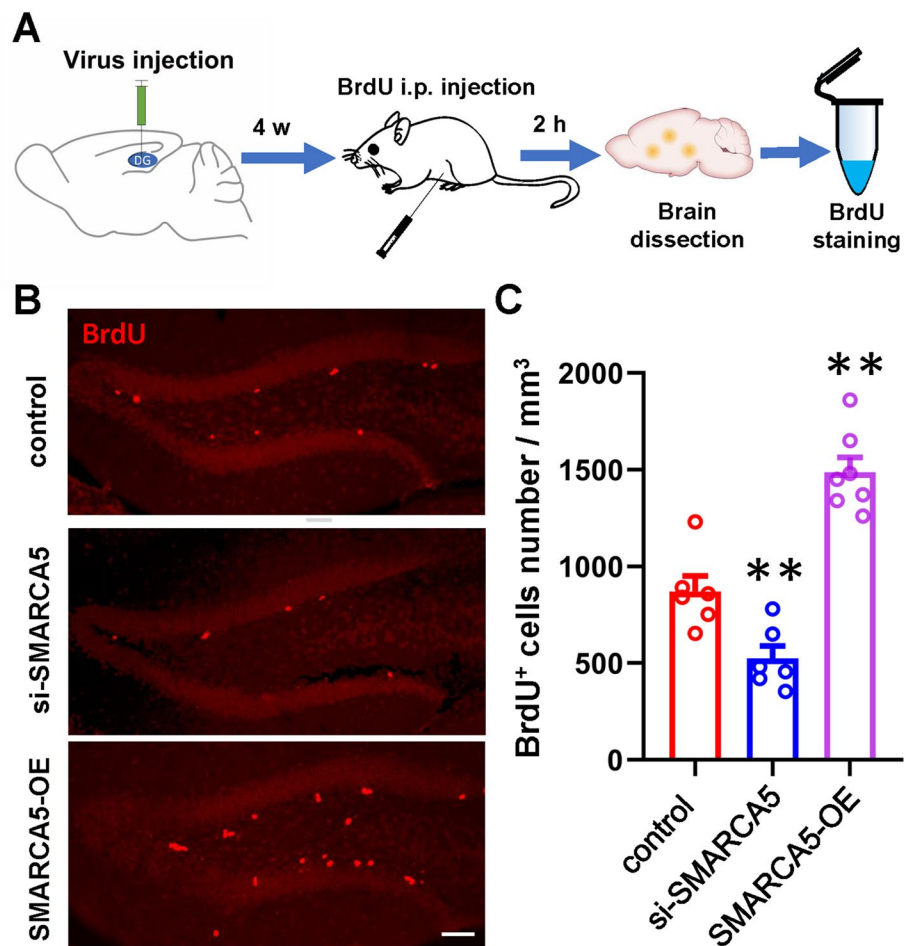


**Fig. 3** Decreasing SMARCA5 impairs the recognition memory and spatial memory in the DG. **A–D** Mice injected with si-SMARCA5 AAV-virus exhibit impaired recognition memory in the novel object recognition test. **(A)** Schematic of the novel object recognition test. **(B)** Total travel distance of mice during acclimation ( $n = 10–11$  per group). **(C)** Recognition index of mismatch and miR-126-anta mice in the object recognition test ( $n = 10–11$  per group,  $*P < 0.05$  vs control group). **(D)** Total exploration time of mismatch and miR-126-anta mice during the object recognition test ( $n = 10–11$  per group). **E–G**

SMARCA5 knockdown impairs spatial memory in the Morris water maze test. **(E)** The escape latency to find the hidden platform on four consecutive days ( $n = 10–11$  per group,  $*P < 0.05$  vs control group). **(F)** The times of platform crossing in the target quadrant in the probe test ( $n = 10–11$  per group,  $**P < 0.01$  vs control group). **(G)** The time spent in the target quadrant in the probe test ( $n = 10–11$  per group,  $**P < 0.01$  vs control group). All values are presented as the mean  $\pm$  SEM.



**Fig. 4** SMARCA5 is related to hippocampal neurogenesis in adult mice. **A** Schematic of the experimental design for examining the effect of SMARCA5 knockdown or overexpression on neurogenesis in the DG. **B**, **C** Knockdown or overexpression of SMARCA5 impairs or elevates neurogenesis in the DG. **(B)** Representative images showing BrdU<sup>+</sup> cells in the DG. Scale bar, 200  $\mu$ m. **(C)** Quantification of BrdU<sup>+</sup> cells in the DG ( $n = 6-7$  mice per group;  $**P < 0.01$  vs control group). All values are presented as the mean  $\pm$  SEM.



enriched proteins were associated with binding, catalytic activity, and molecular function regulators (Fig. 6A, supplementary data 3). The main MF enrichment of DEPs was 5'-nucleotidase activity, proton transmembrane transporter activity, and RAGE receptor binding (Fig. 6B, supplementary data 3). In the CC category, most of the enriched proteins were related to the cell part, organelle part, organelle, and protein-containing complex (Fig. 6A, supplementary data 3). The main CC enrichment of DEPs was a cofilin-actin rod, mitochondrial membrane, and lamellipodium membrane (Fig. 6B, supplementary data 3).

KEGG pathway analysis revealed that the DEPs were mostly enriched in 20 signaling pathways, which included metabolic pathways, pathways of neurodegeneration - multiple diseases, Alzheimer's disease, biosynthesis of secondary metabolites, and Parkinson's disease (Fig. 6C, supplementary data 4). The main KEGG enrichment of DEPs was MAPK signaling pathway - plant, terpenoid backbone biosynthesis, pertussis, NF- $\kappa$ B signaling pathway, and African trypanosomiasis (Fig. 6D, supplementary data 4). Notably, we found that the KEGG analysis results showed that a total of 15 DEPs were enriched in metabolic pathways, which is far more than the DEPs enriched in

other signaling pathways. The KEGG enrichment revealed that DEPs enriched in Pyrimidine metabolism and Purine metabolism had significant enrichment effects. In the BP category of GO analysis, 72 DEPs were enriched in the metabolic process. These analysis results suggested that the metabolic pathway could be an important signaling pathway regulated by SMARCA5 in the hippocampus-dependent memory process. As shown in Fig. 6D and E, the 15 DEPs enriched in metabolic pathways are hydroxyacylglutathione hydrolase (HAGH), protein O-mannose beta-1,4-N-acetylglucosaminyltransferase (POMGNT2), Macrophage migration inhibitory factor (MIF), heme oxygenase 2 (HMOX2), cytosolic 5'-nucleotidase 3 (NT5C), nucleoside diphosphate kinase 3 (NME3), 3-hydroxy-3-methylglutaryl-Coenzyme A synthase 1 (HMGCS1), Aminoacylase-1 (ACY1), sterol carrier protein 2 (SCP2), Glutamyl-tRNA (GLN), amidotransferase subunit B (GATB), adenosine kinase (ADK), cytosolic 5'-nucleotidase 3 (NT5C3), A ATP synthase peripheral stalk-membrane subunit b (ATP5PB), adenylate cyclase 5 (ADCY5), and NADH dehydrogenase [ubiquinone] flavoprotein 3 (NDUFV3).

## The Change of Proteins in the Metabolic Pathway After CFC Training Is Regulated by SMARCA5

To determine whether the 15 proteins changed and were regulated by SMARCA5 after CFC training, RT-PCR was used to initially quantify the levels of these proteins. Mice were randomly divided into 3 groups: a non-CFC group (injection of control AAV-virus, without CFC training), a CFC-2 h group (injection of control AAV-virus, mice were sacrificed at 2 h after CFC training), and a si-SMARCA5+CFC group (injection of si-SMARCA5 AAV-virus, mice were sacrificed at 2 h after CFC training). Our results demonstrated that the mRNA levels of 13 proteins changed significantly in the CFC-2 h group compared with the non-CFC group (*HAGH*, *POMGNT2*, *MIF*, *HMOX2*, *NT5C*, *NME3*, *HMGCS1*, *ACY1*, *SCP2*, *GATB*, *ADK*, *NT5C3*, and *NDUFV3*) (Fig. 7A–L and O; *HAGH*:  $F_{(2,15)} = 4.883$ ,  $P = 0.023$ ; *POMGNT2*:  $F_{(2,15)} = 8.612$ ,  $P = 0.0032$ ; *MIF*:  $F_{(2,15)} = 24.55$ ,  $P < 0.001$ ; *HMOX2*:  $F_{(2,15)} = 12.99$ ,  $P < 0.001$ ; *NT5C*:  $F_{(2,15)} = 9.151$ ,  $P < 0.001$ ; *NME3*:  $F_{(2,15)} = 43.00$ ,  $P < 0.001$ ; *HMGCS1*:  $F_{(2,15)} = 15.56$ ,  $P < 0.001$ ; *ACY1*:  $F_{(2,15)} = 27.23$ ,  $P < 0.001$ ; *SCP2*:  $F_{(2,15)} = 20.55$ ,  $P < 0.001$ ; *GATB*:  $F_{(2,15)} = 13.34$ ,  $P < 0.001$ ; *ADK*:  $F_{(2,15)} = 58.61$ ,  $P < 0.001$ ; *NT5C3*:  $F_{(2,15)} = 54.85$ ,  $P < 0.001$ ; *NDUFV3*:  $F_{(2,15)} = 25.92$ ,  $P < 0.001$ , one-way ANOVA) and the remaining 2 did not exhibit any difference between the two groups of mice (Fig. 7M, N), which suggested that the 13 proteins in the metabolic pathway could be involved in CFC memory formation. Moreover, 8 of these 13 proteins were differentially expressed between the CFC-2 h group and the si-SMARCA5+CFC group (*MIF*, *HMOX2*, *NME3*, *HMGCS1*, *ACY1*, *SCP2*, *ADK*, and *NDUFV3*) (Fig. 7C, D, E, F, G, H, I, J, K, O; *Mif*:  $P = 0.022$ ; *Hmx2*:  $P = 0.011$ ; *Nme3*:  $P < 0.001$ ; *Hmgcs1*:  $P = 0.0094$ ; *Acyl1*:  $P = 0.0056$ ; *Scp2*:  $P = 0.022$ ; *Adk*:  $P < 0.001$ ; *Ndufv3*:  $P = 0.0045$ , two-tailed  $t$  test), suggesting that these 8 proteins in the metabolic pathway could be regulated by SMARCA5 after CFC training.

## The Effect of SMARCA5 on the Maintenance of the Contextual Fear Memory Depends on Metabolic Pathway

The above data indicated that SMARCA5 could modulate the transcription of the 8 proteins in the metabolic pathway after the CFC training; however, whether the 8 proteins are functionally involved in hippocampus-dependent memory and whether the effect of SMARCA5 on CFC memory formation depends on these proteins remained unknown. Given that the 8 proteins in the metabolic pathway we screened out were too many to follow up on, so we decided to select two for further study. We finally chose ACY1 and NME3 by consulting the literature and comprehensively considering their

expression levels in the hippocampus, novelty and importance. Western blot results showed that the protein levels of both ACY1 and NME3 increased at 2 h after CFC training (Fig. 8A, B, C; ACY1:  $F_{(3,19)} = 30.05$ ,  $P < 0.001$ ; NME3:  $F_{(3,19)} = 27.97$ ,  $P < 0.001$ , one-way ANOVA), suggesting that ACY1 and NME3 could participate in CFC memory maintenance. However, when knocking down SMARCA5, the increased ACY1 and NME3 protein levels after CFC training were abolished (Fig. 8A, B, C; ACY1:  $F_{(3,19)} = 30.05$ ,  $P < 0.001$ ; NME3:  $F_{(3,19)} = 27.97$ ,  $P < 0.001$ , one-way ANOVA), which suggested that ACY1 and NME3 were regulated by SMARCA5 in the process of CFC memory maintenance. We then examined whether ACY1 and NME3 are functionally involved in hippocampus-dependent memory. To this end, we used a si-ACY1 AAV-virus and a si-NME3 AAV-virus which simultaneously expressed GFP protein to knock down ACY1 or NME3 levels in the DG. ACY1-overexpression (ACY1-OE) and NME3-overexpression (NME3-OE) AAV-virus, which encoded ACY1 or NME3, and simultaneously expressed GFP protein, were used to overexpress ACY1 or NME3. As shown in Fig. 8A, B, C, mice in the si-SMARCA5+CFC+AAV-OE group (injection of both si-SMARCA5 AAV-virus and ACY1-OE or NME3-OE AAV-virus and sacrificed at 2 h after CFC training) exhibited significantly higher ACY1 and NME3 protein expression than mice in the si-SMARCA5+CFC group (Fig. 8A, B, C; ACY1:  $P < 0.001$ ; NME3:  $P = 0.0015$ , two-tailed  $t$  test), which showed that the AAV-OE virus significantly enhanced the ACY1 and NME3 protein levels.

Next, we subjected mice to CFC training and testing to examine the function of ACY1 and NME3 in hippocampal memory. We first examined the synergistic effect of ACY1 and NME3 on CFC memory. For this purpose, we randomly divided mice into 9 groups: control, si-ACY1, si-NME3, si-ACY1+si-NME3, ACY1-OE, NME3-OE, ACY1-OE+NME3-OE, si-SMARCA5+ACY1-OE+NME3-OE, and SMARCA5-OE+si-ACY1+si-NME3 groups. Mice injected with si-ACY1 and si-NME3 in the DG exhibited intact freezing responses when compared with control mice during CFC training and 1 h after training (Fig. 8D, E), which suggested that knockdown of ACY1 or NME3 had no effects on contextual fear memory acquisition and STM. However, when tested 24 h after training, mice were injected with si-ACY1, si-NME3, or si-ACY1+si-NME3 exhibited less freezing time than mice in the control group (Fig. 8E;  $F_{(4,53)} = 27.97$ ,  $P < 0.001$ , one-way ANOVA), suggesting that knockdown of ACY1 and NME3 impairs the hippocampal contextual fear LTM. Meanwhile, mice in the ACY1-OE, NME3-OE, and ACY1-OE+NME3-OE groups showed an intact freezing time during training and the STM test, but a significantly increased freezing time during the LTM test compared with mice in the control group (Fig. 8F, G;  $F_{(4,51)} = 5.518$ ,  $P < 0.001$ , one-way ANOVA), which suggested

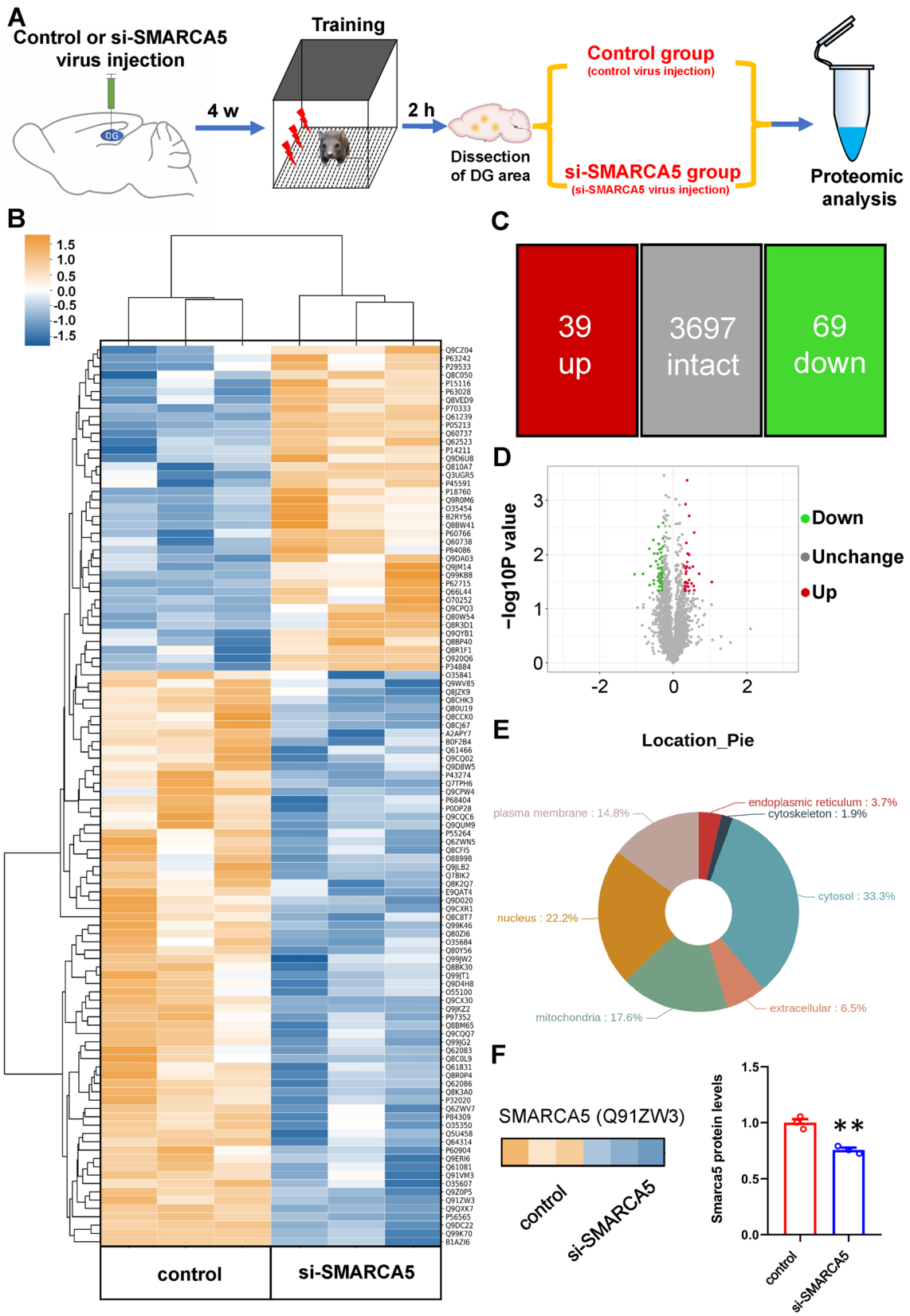


**Fig. 5** Proteomics analysis of the effects of SMARCA5 knockdown on protein changes in the DG after CFC training. **A** Schematic of the experimental design for proteomics analysis. **B** Heatmap results reveal protein levels in the DG of mice in the control group compared with mice in the si-SMARCA5 group (blue-white-yellow: low-to-high protein levels). **C, D** Proteomics results for protein fold changes in the DG ( $P < 0.05$ ). **E** Analysis results of the subcellular localization of differentially expressed proteins. **F** Proteomics results of SMARCA5 protein levels in the DG ( $n = 3$  per group;  $**P < 0.01$  vs control group). All values are presented as the mean  $\pm$  SEM.

that overexpression of ACY1 and NME3 enhances the hippocampal contextual fear LTM. Taken together, these results indicate that ACY1 and NME3 are essential for the maintenance of hippocampal contextual fear LTM.

We then asked whether the effect of SMARCA5 on CFC memory formation depended on ACY1 and NME3. The results above revealed that overexpressing SMARCA5 increased CFC LTM formation (Fig. 2G), and mice in the si-ACY1+si-NME3 group exhibited a reduced freezing time when compared with mice in the control group (Fig. 8E,  $P < 0.001$ , two-tailed  $t$  test), suggesting that blocking ACY1 and NME3 suppressed the contextual fear LTM. However, freezing time was significantly lower in the SMARCA5-OE+si-ACY1+si-NME3 group than that in the control group (Fig. 8E,  $P < 0.001$ , two-tailed  $t$  test). By contrast, no significant differences were found compared with that of the si-ACY1+si-NME3 group (Fig. 8E), which suggested that impaired ACY1 and NME3 functions can block the enhancement of SMARCA5-induced contextual fear memory maintenance. Moreover, mice in the si-SMARCA5+ACY1-OE+NME3-OE group exhibited significantly more freezing time than mice in the control group (Fig. 8G,  $P < 0.001$ , two-tailed  $t$  test) and did not significantly differ from mice in the ACY1-OE+NME3-OE group (Fig. 8G), suggesting that the suppressed SMARCA5 function in CFC memory can be rescued by elevating of ACY1 and NME3. These results revealed that the effect of SMARCA5 on the CFC memory in the DG depends on the proteins ACY1 and NME3 of the metabolic pathway.

## Discussion

In this study, we demonstrated that SMARCA5 is responsible for hippocampal contextual fear memory maintenance and adult neurogenesis. Using proteomics analysis, we revealed the proteins that were modulated by SMARCA5 during the processes of CFC memory and the signaling pathways that these proteins are enriched for. Moreover, we found that multiple proteins in metabolic pathways are regulated by SMARCA5 after CFC training. Finally, we indicated that SMARCA5 regulates its target ACY1 and

NME3 protein levels in metabolic pathways to facilitate the maintenance of hippocampal fear memory.

Our data provide several new insights into the mechanisms of chromatin remodeling in hippocampus-dependent memory. First, we revealed that SMARCA5 is essential for hippocampus-dependent memory and adult neurogenesis. As a chromatin remodeling factor, SMARCA5 forms ordered nucleosome arrays on chromatin and promotes access to DNA during DNA-templated processes such as DNA transcription, replication, and repair [30–33]. Picketts' group revealed that SMARCA5 conditional KO mice with a Nestin-Cre driver line exhibit a reduced brain size with striking cerebellar hypoplasia and signs of premature death. The cerebellar hypoplasia leads to poor motor function and impaired associative learning skills [19]. A recent study indicated that the SMARCA5 expression in the amygdala and ventral hippocampus is reduced in mice with high anxiety-related behavior [21], however, currently, the roles of SMARCA5 in adult learning and memory are still unclear. Our data demonstrated that SMARCA5 levels in the dorsal DG, but not the ventral DG and BLA, increased after CFC training, whereas blocking SMARCA5 impaired hippocampus-dependent memory and adult neurogenesis. Moreover, overexpression of SMARCA5 elevated contextual fears of LTM and adult neurogenesis. Thus, these results indicate that SMARCA5 is necessary and sufficient for contextual fears of LTM and adult neurogenesis. The role of hippocampal neurogenesis in hippocampal memory is quite complicated, and there are still some controversies on this issue. The continued integration of new neurons into hippocampal circuits throughout adulthood has been hypothesized to affect memory function in two ways [34]. First, newly integrated neurons provide fresh substrates for learning and thus may facilitate the maintenance of new memories (for example, by increasing capacity or allowing more efficient pattern separation). This hypothesis is supported by studies showing that inhibition of hippocampal neurogenesis generally impairs memory maintenance [35–37] while promoting hippocampal neurogenesis improves memory maintenance [38–40]. Second, by modifying the pattern of input and output connections in the DG, the integration of new neurons alters hippocampal circuits, thus potentially making memories already stored in these circuits more difficult to access at later time points. However, it is still unclear whether SMARCA5-mediated neurogenesis is a key factor leading to changes in hippocampal learning and memory, and this question still requires follow-up research.

Second, we used proteomics to analyze the proteins that were modulated by SMARCA5 during the process of CFC memory maintenance and the signaling pathways that these proteins are enriched for. As a chromatin remodeling factor, the transcription and expression of a huge number of proteins could be regulated by SMARCA5. However, which



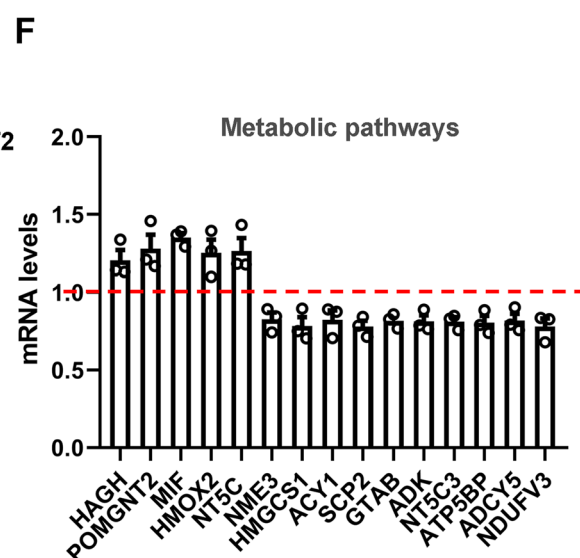
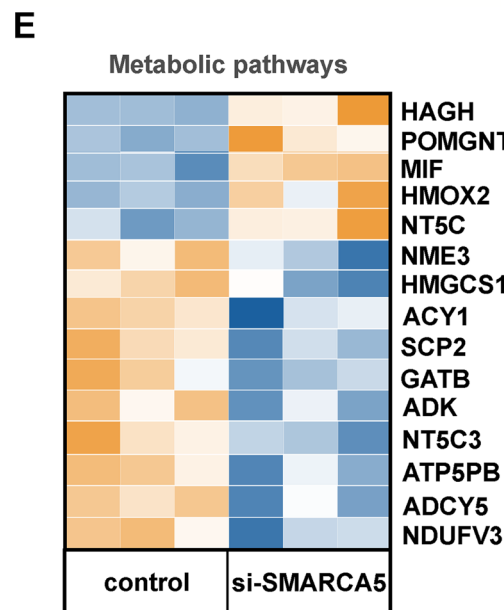
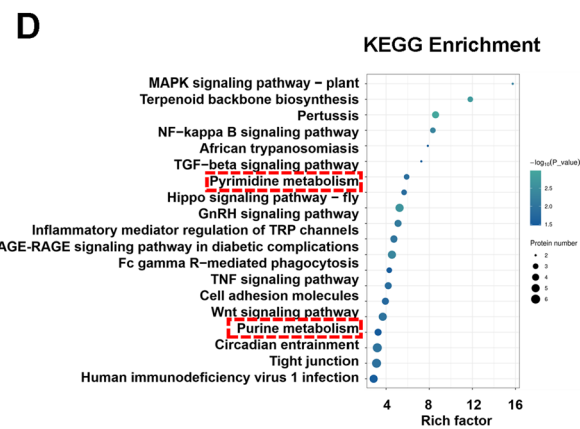
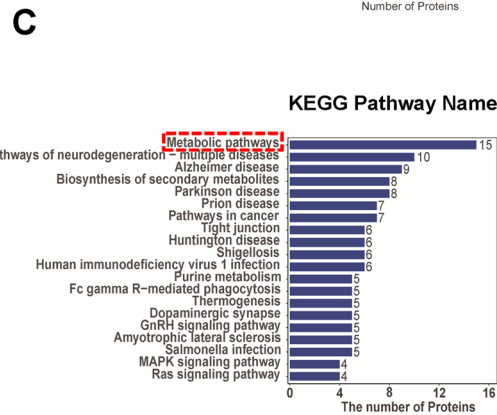
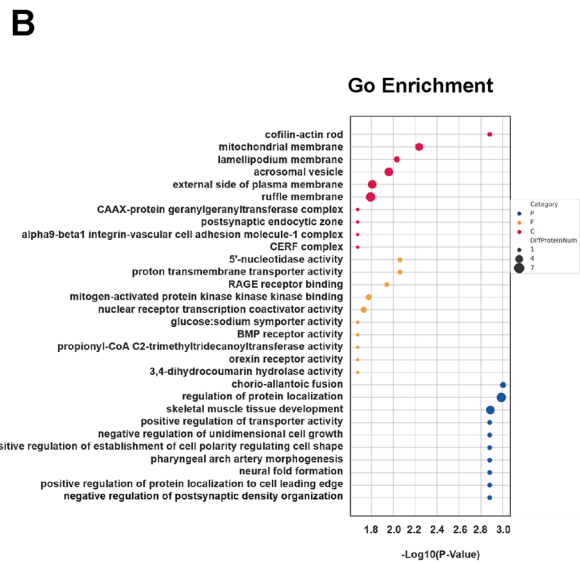
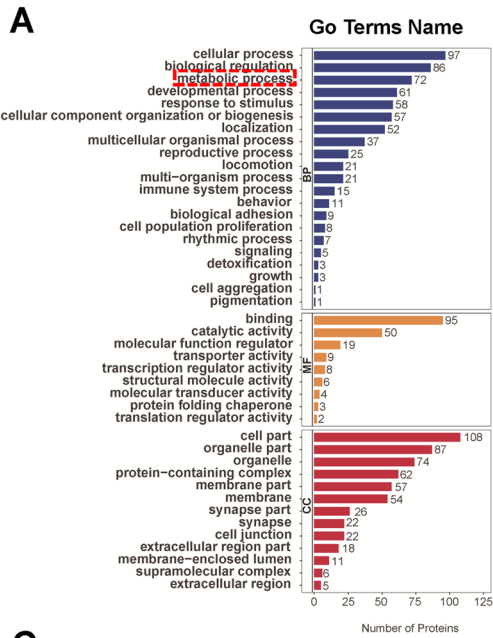




**Fig. 6** GO and KEGG analysis to determine the signaling pathways and enrichment of the DEPs. **A** GO terms analysis of the DEPs in the DG. **B** Pathway enrichment in the dot plot. The colors of the dots represent the different categories and the sizes of the nodes represent the number of DEPs in the pathway. **C** KEGG pathway analysis of the DEPs in the DG. **D** Pathway enrichment in the dot plot. The colors of the dots and their sizes are as above. **E** Heatmap results reveal proteins in the metabolic pathway of mice in the control group compared with mice in the si-SMARCA5 group (blue-white-yellow: low-to-high protein levels). **F** Relative densitometric analysis of proteins in the metabolic pathway ( $P < 0.05$ ).

specific proteins and signaling pathways were regulated by SMARCA5 in response to memory formation during the hippocampus-dependent memory process? The classical one-to-one research method of finding downstream target genes is more refined and accurate, but it is inefficient and incomplete. In the age of systems biology and bioinformatics, high-throughput analysis is more efficient and can comprehensively dissect the entire regulatory network from a holistic perspective. By using proteomics analysis, we

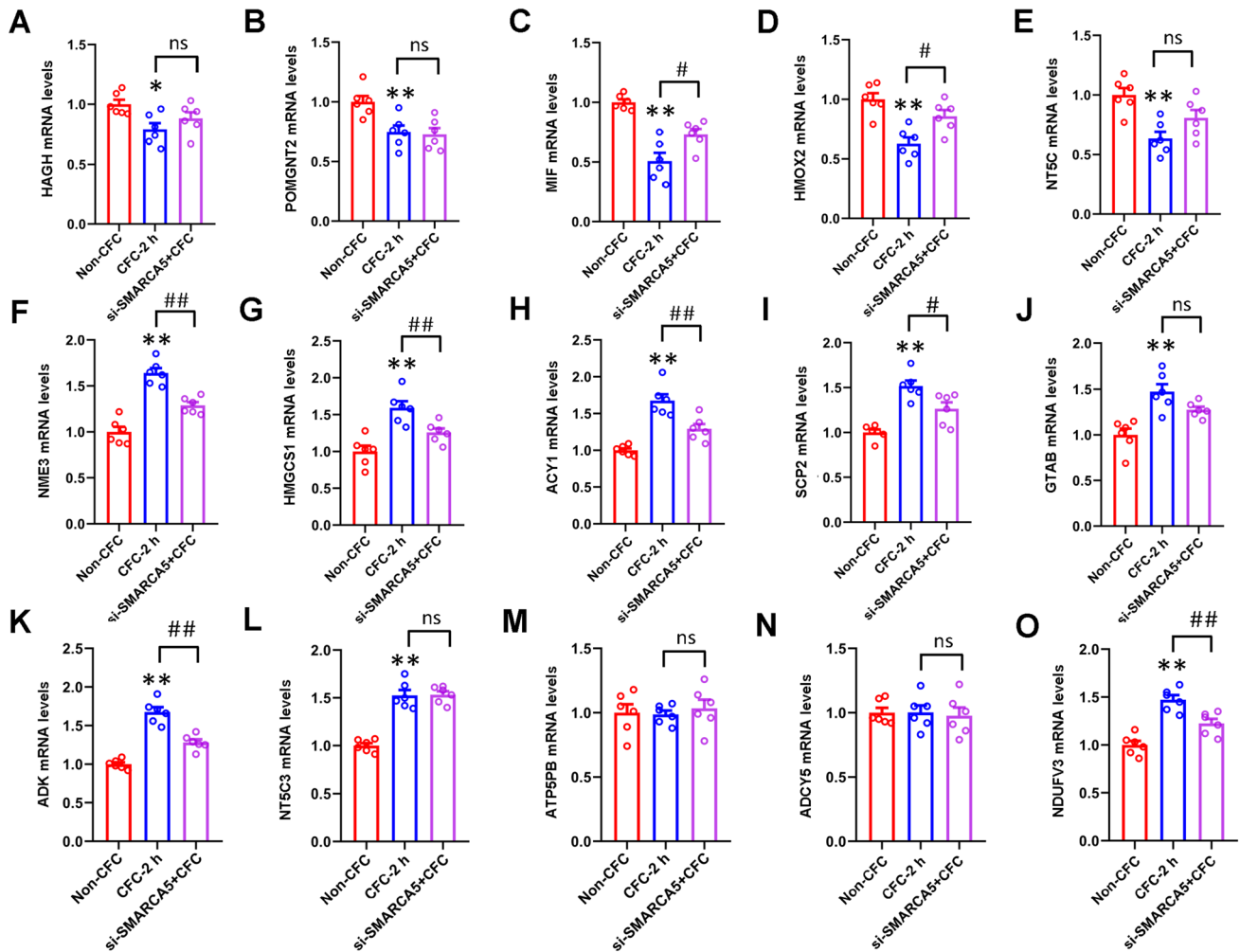


**Fig. 7** The effects of SMARCA5 knockdown on the mRNA changes of metabolic pathway-related proteins after CFC training. **A–O** The relative mRNA levels of metabolic pathway-related proteins in the non-CFC, CFC-2 h, and Si-SMARCA5+CFC groups. **(A)** The relative *HAGH* mRNA levels ( $n = 6$  mice per group;  $*P < 0.05$  vs non-CFC group). **(B)** The relative *POMGNT2* mRNA levels ( $n = 6$  mice per group;  $**P < 0.01$  vs non-CFC group). **(C)** The relative *MIF* mRNA levels ( $n = 6$  mice per group;  $**P < 0.01$  vs non-CFC group). **(D)** The relative *HMOX2* mRNA levels ( $n = 6$  mice per group;  $**P < 0.01$  vs non-CFC group). **(E)** The relative *NT5C* mRNA levels ( $n = 6$  mice per group;  $**P < 0.01$  vs non-CFC group). **(F)** The relative *NME3* mRNA levels ( $n = 6$  mice per group;  $**P < 0.01$  vs Non-CFC group). **(G)** The relative *HMGCS1* mRNA levels ( $n = 6$  mice

per group;  $**P < 0.01$  vs non-CFC group). **(H)** The relative *ACY1* mRNA levels ( $n = 6$  mice per group;  $**P < 0.01$  vs non-CFC group). **(I)** The relative *SCP2* mRNA levels ( $n = 6$  mice per group;  $**P < 0.01$  vs non-CFC group). **(J)** The relative *GATB* mRNA levels ( $n = 6$  mice per group;  $**P < 0.01$  vs non-CFC group). **(K)** The relative *ADK* mRNA levels ( $n = 6$  mice per group;  $**P < 0.01$  vs non-CFC group). **(L)** The relative *NT5C3* mRNA levels ( $n = 6$  mice per group;  $*P < 0.05$  vs non-CFC group). **(M)** The relative *Atp5pb* mRNA levels ( $n = 6$  mice per group). **(N)** The relative *ADCY5* mRNA levels ( $n = 6$  mice per group). **(O)** The relative *NDUFV3* mRNA levels ( $n = 6$  mice per group;  $*P < 0.05$  vs non-CFC group). All values are presented as the mean  $\pm$  SEM.

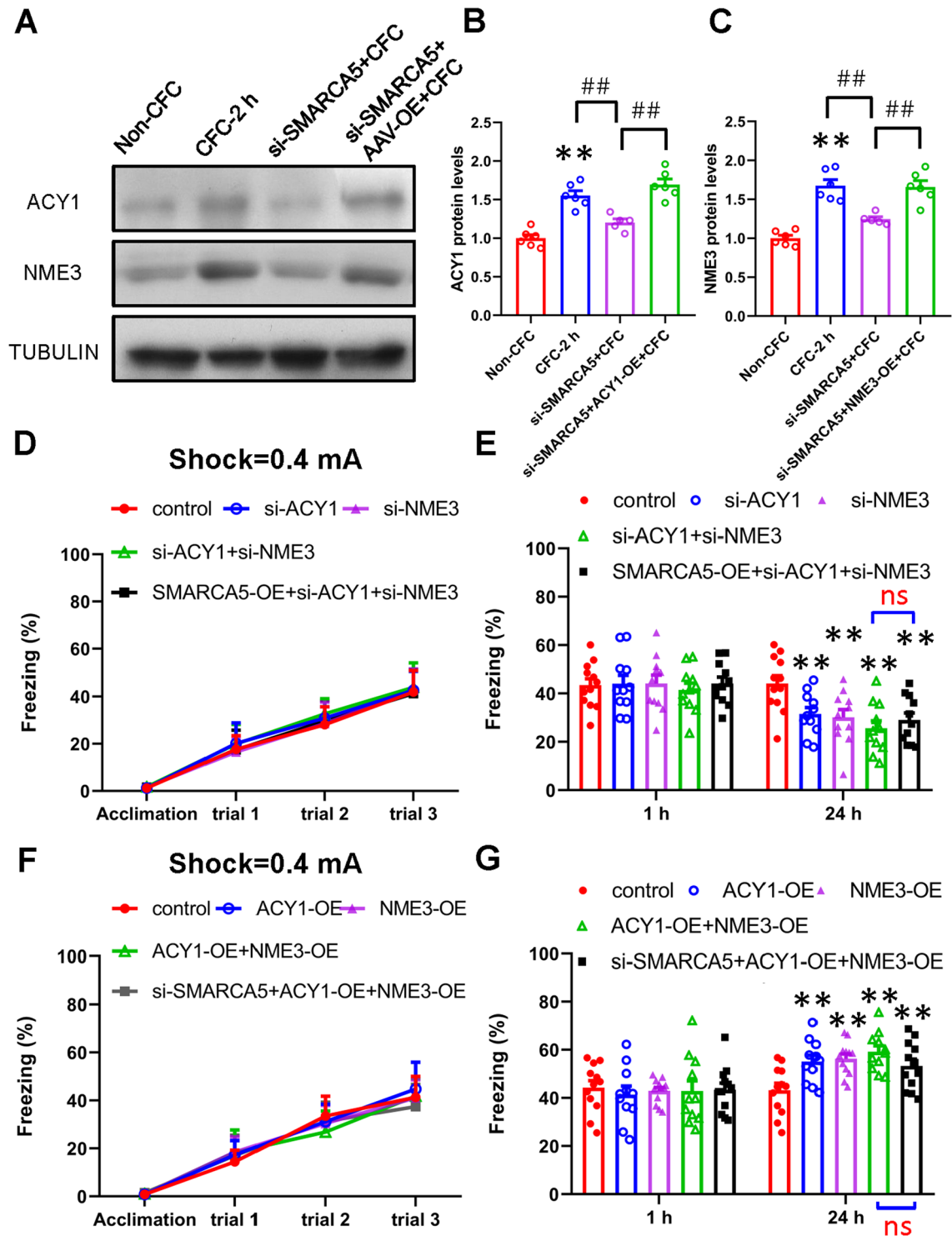


**Fig. 8** The effect of SMARCA5 on contextual fear memory depends on the metabolic pathway. **A–C** Representative immunoblots and the relative densitometric analysis of NME3 and ACY1 in the non-CFC, CFC-2 h, si-SMARCA5+CFC, and si-SMARCA5+AAV-OE+CFC groups. Representative immunoblots are shown in **(A)**, and the relative densitometric analysis is shown in **B** and **C**,  $n = 5–6$  per group;  $***P < 0.01$  vs non-CFC group. **D, E** The effect of SMARCA5 on contextual fear memory depends on ACY1. **(D)** The freezing response in

the training process. **(E)** The freezing response at 1 h and 24 h after training ( $n = 11–12$  per group;  $**P < 0.01$  vs control group). **F, G** The effect of SMARCA5 on contextual fear memory depends on NME3. **(F)** The freezing response in the training process. **(G)** The freezing response at 1 h and 24 h after training ( $n = 11–12$  per group;  $**P < 0.01$  vs control group). All values are presented as the mean  $\pm$  SEM.

revealed the proteins regulated by SMARCA5 in the process of CFC memory formation and analyzed the signaling pathways enriched by these proteins using the GO and KEGG signaling pathways, which provides data references and analysis for subsequent researchers.

Finally, our results indicated that SMARCA5 participates in hippocampal contextual fear memory by targeting ACY1 and NME3. The metabolic pathway is a large and complex network of signaling pathways, which is an indispensable part of the body, but its functions in learning and memory are less studied. Our proteomics analysis, RT-PCR, and western blot all showed that knockdown of SMARCA5 impaired the increased expression of ACY1 and NME3 2 h after CFC training. Data concerning behavior showed that down-regulating ACY1 and NME3 together impaired the contextual fear memory, but SMARCA5 overexpression did not reverse the ACY1 and NME3 downregulation-induced memory deficits. Moreover, up-regulating ACY1 and NME3 together did elevate the contextual fear LTM, and SMARCA5 overexpression did not impair the ACY1 and NME3 upregulation-induced memory enhancement. Thus, these results indicated that the participation of SMARCA5 in hippocampus-dependent memory depends on its targets, ACY1 and NME3. As an important zinc-binding enzyme in the signaling pathway, ACY1 catalyzes the hydrolysis of acylated L-amino acids to L-amino acids and an acyl group. The expression of ACY1 has been reported to be reduced in SCLC cell lines and tumors [41]. Although studies have shown that mutations in ACY1 cause aminoacylase-1 deficiency, a metabolic disorder characterized by central nervous system defects and increased urinary excretion of N-acetylated amino acids [42, 43], the functions of ACY1 in the brain have hardly been studied. Since the main functions of Acy-1 are to accelerate the hydrolysis of N-acetylated peptides, especially N-acetylated neutral aliphatic amino acids, and participate in protein synthesis through the release of free amino acids, ACY1 may be involved in hippocampal memory by affecting protein synthesis. NME3, which is a member of the nucleoside diphosphate kinase family that binds to the mitochondrial outer membrane to stimulate mitochondrial fusion [44], provides GTP to the GTP-requiring proteins localized in peroxisomes and mitochondria. NME3 is involved in a variety of cellular processes, including signal transduction, development, cancer metastasis, and metabolism. Recent studies have shown that NME3 regulates mitochondrial dynamics and is important for neuronal survival [45, 46]; in this case, NME3 may participate in learning and memory by regulating mitochondrial function. Future studies may help to elucidate the mechanisms by which ACY1 and NME3 are involved in learning and memory.

In conclusion and to the best of our knowledge, this work is the first to determine that SMARCA5 is involved in adult hippocampal memory maintenance and neurogenesis. Evidence is provided to reveal the proteins and signaling

pathways that were affected by SMARCA5 knockdown during the CFC formation process. Finally, we found that SMARCA5 participated in hippocampal contextual fear memory formation by regulating proteins in metabolic pathways such as ACY1 and NME3. Our study enhances the understanding of chromatin remodeling in learning and memory. Considering that chromatin remodeling is essential for many brain disorders, we recommend further studies on SMARCA5 as a potentially important therapeutic target.

**Acknowledgments** This work was supported by the Youth Program of the National Natural Science Foundation of China (32000788); Shandong Province Natural Science Foundation (ZR2019 BC097); Key Project from the National Natural Science Foundation of China (81830035); the Major program of National Natural Science Foundation of China (82090033); the Major Basic research program of Shandong Province Natural Science Foundation (ZR2019ZD35); The Major program of Technological innovation 2030 “Brain science and brain-inspired research” (2021ZD0203002); Shandong Taishan Scholar Award; and the Fundamental Research Funds of Qingdao University.

**Conflict of Interest** The authors declare that there are no conflicts of interest.

## References

1. Marco A, Meharena HS, Dileep V, Raju RM, Davila-Velderrain J, Zhang AL. Mapping the epigenomic and transcriptomic interplay during memory formation and recall in the hippocampal engram ensemble. *Nat Neurosci* 2020, 23: 1606–1617.
2. Xu XF, Jing X, Ma HX, Yuan RR, Dong Q, Dong JL, *et al.* MiR-181a participates in contextual fear memory formation via activating mTOR signaling pathway. *Cereb Cortex* 2018, 28: 3309–3321.
3. Zovkic IB, Sweatt JD. Epigenetic mechanisms in learned fear: Implications for PTSD. *Neuropsychopharmacology* 2013, 38: 77–93.
4. Dias BG, Maddox S, Klengel T, Ressler KJ. Epigenetic mechanisms underlying learning and the inheritance of learned behaviors. *Trends Neurosci* 2015, 38: 96–107.
5. Cui X, Zhang R, Yang Y, Wu E, Tang Y, Zhao Z, *et al.* Identification and characterization of long non-coding RNA *Carip* in modulating spatial learning and memory. *Cell Rep* 2022, 38: 110398.
6. Yoon G, Lim YH, Jo D, Ryu J, Song J, Kim YK. Obesity-linked circular RNA circTshz2-2 regulates the neuronal cell cycle and spatial memory in the brain. *Mol Psychiatry* 2021, 26: 6350–6364.
7. Griggs EM, Young EJ, Rumbaugh G, Miller CA. MicroRNA-182 regulates amygdala-dependent memory formation. *J Neurosci* 2013, 33: 1734–1740.
8. Vergallo A, Lista S, Zhao Y, Lemercier P, Teipel SJ, Potier MC, *et al.* MiRNA-15b and miRNA-125b are associated with regional A $\beta$ -PET and FDG-PET uptake in cognitively normal individuals with subjective memory complaints. *Transl Psychiatry* 2021, 11: 78.
9. Zhao C, Zhou B, Cao J, Zhang Y, Li W, Wang M, *et al.* MiR-187-3p participates in contextual fear memory formation through modulating SATB2 expression in the hippocampus. *Neuroreport* 2020, 31: 909–917.
10. Jarome TJ, Lubin FD. Histone lysine methylation: Critical regulator of memory and behavior. *Rev Neurosci* 2013, 24: 375–387.
11. Gupta S, Kim SY, Artis S, Molfese DL, Schumacher A, Sweatt JD, *et al.* Histone methylation regulates memory formation. *J Neurosci* 2010, 30: 3589–3599.

12. González-Rodríguez P, Cheray M, Füllgrabe J, Salli M, Engskog-Vlachos P, Keane L, *et al.* The DNA methyltransferase DNMT3A contributes to autophagy long-term memory. *Autophagy* 2021, 17: 1259–1277.
13. Jarome TJ, Perez GA, Webb WM, Hatch KM, Navabpour S, Musaus M, *et al.* Ubiquitination of histone H2B by proteasome subunit RPT6 controls histone methylation chromatin dynamics during memory formation. *Biol Psychiatry* 2021, 89: 1176–1187.
14. Kim S, Yu NK, Shim KW, Kim JI, Kim H, Han DH, *et al.* Remote memory and cortical synaptic plasticity require neuronal CCCTC-binding factor (CTCF). *J Neurosci* 2018, 38: 5042–5052.
15. Schoberleitner I, Mutti A, Sah A, Wille A, Gimeno-Valiente F, Piatti P, *et al.* Role for chromatin remodeling factor Chd1 in learning and memory. *Front Mol Neurosci* 2019, 12: 3.
16. Zhao XC, An P, Wu XY, Zhang LM, Long B, Tian Y, *et al.* Overexpression of hSNF2H in glioma promotes cell proliferation, invasion, and chemoresistance through its interaction with Rsf-1. *Tumour Biol* 2016, 37: 7203–7212.
17. Sheu JJ, Choi JH, Yildiz I, Tsai FJ, Shaul Y, Wang TL, *et al.* The roles of human sucrose nonfermenting protein 2 homologue in the tumor-promoting functions of Rsf-1. *Cancer Res* 2008, 68: 4050–4057.
18. Alvarez-Saavedra M, Yan K, De Repentigny Y, Hashem LE, Chaudary N, Sarwar S, *et al.* Snf2h drives chromatin remodeling to prime upper layer cortical neuron development. *Front Mol Neurosci* 2019, 12: 243.
19. Alvarez-Saavedra M, De Repentigny Y, Lagali PS, Raghu Ram EVS, Yan K, Hashem E, *et al.* Snf2h-mediated chromatin organization and histone H1 dynamics govern cerebellar morphogenesis and neural maturation. *Nat Commun* 2014, 5: 4181.
20. Alvarez-Saavedra M, De Repentigny Y, Yang D, O'Meara RW, Yan K, Hashem LE, *et al.* Voluntary running triggers VGF-mediated oligodendrogenesis to prolong the lifespan of Snf2h-null ataxic mice. *Cell Rep* 2016, 17: 862–875.
21. Wille A, Amort T, Singewald N, Sartori SB, Lusser A. Dysregulation of select ATP-dependent chromatin remodeling factors in high trait anxiety. *Behav Brain Res* 2016, 311: 141–146.
22. Paizanis E, Renoir T, Lelievre V, Saurini F, Melfort M, Gabriel C, *et al.* Behavioural and neuroplastic effects of the new-generation antidepressant agomelatine compared to fluoxetine in glucocorticoid receptor-impaired mice. *Int J Neuropsychopharmacol* 2010, 13: 759–774.
23. Jing X, Sui WH, Wang S, Xu XF, Yuan RR, Chen XR, *et al.* HDAC7 ubiquitination by the E3 ligase CBX4 is involved in contextual fear conditioning memory formation. *J Neurosci* 2017, 37: 3848–3863.
24. O'Leary OF, O'Connor RM, Cryan JF. Lithium-induced effects on adult hippocampal neurogenesis are topographically segregated along the dorso-ventral axis of stressed mice. *Neuropharmacology* 2012, 62: 247–255.
25. Papatheodoropoulos C. Higher intrinsic network excitability in ventral compared with the dorsal hippocampus is controlled less effectively by GABAB receptors. *BMC Neurosci* 2015, 16: 75.
26. Xue B, Qu Y, Zhang X, Xu XF. miRNA-126a-3p participates in hippocampal memory *via* alzheimer's disease-related proteins. *Cereb Cortex* 2022, 32: 4763–4781.
27. Xu XF, Wang YC, Zong L, Chen ZY, Li Y. Elevating Integrin-linked Kinase expression has rescued hippocampal neurogenesis and memory deficits in an AD animal model. *Brain Res* 2018, 1695: 65–77.
28. West MJ, Gundersen HJ. Unbiased stereological estimation of the number of neurons in the human hippocampus. *J Comp Neurol* 1990, 296: 1–22.
29. Lybrand ZR, Goswami S, Zhu J, Jarzabek V, Merlock N, Aktar M, *et al.* A critical period of neuronal activity results in aberrant neurogenesis rewiring hippocampal circuitry in a mouse model of epilepsy. *Nat Commun* 2021, 12: 1423.
30. Poot RA, Dellaire G, Hülsmann BB, Grimaldi MA, Corona DF, Becker PB, *et al.* HuCHRAC, a human ISWI chromatin remodeling complex contains hACF<sub>1</sub> and two novel histone-fold proteins. *EMBO J* 2000, 19: 3377–3387.
31. Oppikofer M, Bai T, Gan Y, Haley B, Liu P, Sandoval W, *et al.* Expansion of the ISWI chromatin remodeler family with new active complexes. *EMBO Rep* 2017, 18: 1697–1706.
32. Hakimi MA, Bochar DA, Schmiesing JA, Dong Y, Barak OG, Speicher DW, *et al.* A chromatin remodelling complex that loads cohesin onto human chromosomes. *Nature* 2002, 418: 994–998.
33. Loyola A, Huang JY, LeRoy G, Hu S, Wang YH, Donnelly RJ, *et al.* Functional analysis of the subunits of the chromatin assembly factor RSF. *Mol Cell Biol* 2003, 23: 6759–6768.
34. Frankland PW, Köhler S, Josselyn SA. Hippocampal neurogenesis and forgetting. *Trends Neurosci* 2013, 36: 497–503.
35. Ko HG, Jang DJ, Son J, Kwak C, Choi JH, Ji YH, *et al.* Effect of ablated hippocampal neurogenesis on the formation and extinction of contextual fear memory. *Mol Brain* 2009, 2: 1.
36. Zhuo JM, Tseng HA, Desai M, Bucklin ME, Mohammed AI, Robinson NT, *et al.* Young adult born neurons enhance hippocampal dependent performance *via* influences on bilateral networks. *eLife* 2016, 5: e22429.
37. Clelland CD, Choi M, Romberg C, Clemenson GD Jr, Fragniere A, Tyers P, *et al.* A functional role for adult hippocampal neurogenesis in spatial pattern separation. *Science* 2009, 325: 210–213.
38. Xu XF, Li T, Wang DD, Chen B, Wang Y, Chen ZY. Integrin-linked kinase is essential for environmental enrichment enhanced hippocampal neurogenesis and memory. *Sci Rep* 2015, 5: 11456.
39. Sahay A, Scobie KN, Hill AS, O'Carroll CM, Kheirbek MA, Burghardt NS, *et al.* Increasing adult hippocampal neurogenesis is sufficient to improve pattern separation. *Nature* 2011, 472: 466–470.
40. Creer DJ, Romberg C, Saksida LM, van Praag H, Bussey TJ. Running enhances spatial pattern separation in mice. *Proc Natl Acad Sci U S A* 2010, 107: 2367–2372.
41. Cook RM, Burke BJ, Buchhagen DL, Minna JD, Miller YE. Human aminoacylase-1. Cloning, sequence, and expression analysis of a chromosome 3p21 gene inactivated in small cell lung cancer. *J Biol Chem* 1993, 268: 17010–17017.
42. Sass JO, Vaithilingam J, Gemperle-Britschgi C, Delnooz CC, Kluijtmans LA, van de Warrenburg BP, *et al.* Expanding the phenotype in aminoacylase 1 (ACY1) deficiency: Characterization of the molecular defect in a 63-year-old woman with generalized dystonia. *Metab Brain Dis* 2016, 31: 587–592.
43. Tytki-Szymanska A, Gradowska W, Sommer A, Heer A, Walter M, Reinhard C, *et al.* Aminoacylase 1 deficiency associated with autistic behavior. *J Inher Metab Dis* 2010, 33: 211–214.
44. Chen CW, Tsao N, Zhang W, Chang ZF. NME3 regulates mitochondria to reduce ROS-mediated genome instability. *Int J Mol Sci* 2020, 21: 5048.
45. Chen CW, Wang HL, Huang CW, Huang CY, Lim WK, Tu IC, *et al.* Two separate functions of NME3 critical for cell survival underlie a neurodegenerative disorder. *Proc Natl Acad Sci U S A* 2019, 116: 566–574.
46. Wertz MH, Mitchem MR, Pineda SS, Hachigian LJ, Lee H, Lau V, *et al.* Genome-wide *in vivo* CNS screening identifies genes that modify CNS neuronal survival and mHTT toxicity. *Neuron* 2020, 106: 76–89.e8.

Springer Nature or its licensor (e.g. a society or other partner) holds exclusive rights to this article under a publishing agreement with the author(s) or other rightsholder(s); author self-archiving of the accepted manuscript version of this article is solely governed by the terms of such publishing agreement and applicable law.